

PRIORITY COMMUNICATION

Oscillatory Driven Cavity with an Air/Water Interface and an Insoluble Monolayer: Surface Viscosity Effects

Juan M. Lopez* and Amir H. Hirsaj†

*Department of Mathematics, Arizona State University, Tempe, Arizona 85287-1804; and †Department of Mechanical Engineering, Aeronautical Engineering, and Mechanics, Rensselaer Polytechnic Institute, Troy, New York 12180-3590

Received April 5, 2001; accepted July 30, 2001

Flow in a planar cavity bounded by stationary side walls, a flat gas/liquid interface covered by an insoluble monolayer, and driven by sinusoidal motion of the floor is examined numerically. Navier–Stokes computations with the Boussinesq–Scriven surface model are presented utilizing the equation-of-state measured for a vitamin K₁ monolayer on the air/water interface. The results identify a range of initial surfactant concentration for which the surface velocity is sensitive to the surface viscosity \mathcal{B} (sum of surface shear and dilatational viscosities) down to 10^{-2} surface Poise. Thus, the study suggests a practical method for determining surface viscosities consisting of the measurement of the motion of a tracer particle on the interface and comparisons with numerical computations at various values of \mathcal{B} . © 2001 Academic Press

Key Words: insoluble surfactants; nonlinear equation-of-state; surface dilatational viscosity.

1. INTRODUCTION

There is much interest in gas/liquid interfaces, e.g., air/water, due in part to the recent interest in microfluidic systems, which are gaining technological importance. When there is a free surface in the system (which in some cases is unavoidable, especially when channel walls are not fully wetting, and in many cases essential, e.g., for gas analysis using microchannels), then the coupling between the interface and the bulk flow needs to be considered. When the length scales are small, then interfacial effects can dominate effects of gravity and other forces. For very small length scales, the effect of intrinsic surface viscosities (surface shear, μ^s , and surface dilatational, κ^s) can dominate the effect of surface elasticity (surface tension gradients). Of the two surface viscosities, surface shear viscosity has been consistently measured for a variety of surfactant systems using different techniques (1, 2). However, the same is not true of the surface dilatational viscosity. Determination of κ^s is difficult since its effects

are coupled to surface tension, both in the normal and tangential stress balances. General agreement between measurements of κ^s with different techniques have yet to be demonstrated (3); results varying by several orders of magnitude have been reported (2), as well as negative values of κ^s (4). Most indications are that κ^s may be many orders of magnitude larger than μ^s (5–8), so it is important to develop techniques to measure it reliably.

Either the tangential or the normal stress balance may be used to determine κ^s . One of the techniques that utilizes the normal stress is the maximum bubble pressure method (9). This technique is not applicable to the measurement of κ^s for insoluble (Langmuir) monolayers, which are of interest to this study. Also, the complexities resulting from gradients in surfactant distribution on the surface of the bubble, e.g., development of shear stress along the surface, have not been addressed and may account for some of the discrepancies seen between different measurements of κ^s . Other methods that try to determine κ^s are drop deformation techniques, but they are not easy to apply to insoluble systems. Although in principle it is possible to spread an insoluble monolayer on an order 1-mm drop, it is difficult to know how much material is present on the surface. Thus, these techniques have been primarily applied to soluble systems (10–12). For larger drops, distortions due to gravity become increasingly important and the technique requires a microgravity environment (13). These techniques all assume spherical symmetry, yet in practice there is always a lip (e.g., in pendant drop, maximum bubble pressure method, etc.), so the role of tangential stress may remain unaccounted for.

The classic example that utilizes the tangential stress balance to determine κ^s is the longitudinal wave method (14). This technique is based on theory that assumes an inertialess limit, hence the restriction to small barrier speed/frequency. Small barrier speed/frequency is also necessary to avoid making transverse waves as the theory is based on an essentially flat interface. When small frequency is used, then the effect of elasticity can

dominate the effect of surface viscosities (the product of Boussinesq number and capillary number being small), so errors in determining elasticity (e.g., deviations in the equation-of-state) may lead to large errors in κ^s . Another method using the tangential stress balance employs a transient vortex flow and simultaneously measures the surfactant concentration on the interface, $c(x, t)$, and the surface velocity, $u^s(x, t)$, at a given location x (8). The problem with the transient vortex method is that the flow is not time-periodic, so one cannot do phase averaging. As a result, there are large inaccuracies (at least 50% noise level) in the determination of surface viscosities. Further, the simultaneous measurement of both c and u^s is technically challenging, especially since nonlinear optics had to be used to measure c .

We propose a cavity-driven flow; by changing from a barrier-driven flow, we can drive the system at higher Reynolds numbers (based on frequency and amplitude) and still avoid complicated surface deformation problems.

2. EQUATIONS GOVERNING THE DRIVEN CAVITY FLOW

The flow consists of fluid of density ρ , molecular viscosity μ (and kinematic viscosity $\nu = \mu/\rho$), contained in a rectangular region of width $2L$ and depth H , and driven by the horizontal harmonic oscillation of the bottom boundary. The top surface of the fluid is exposed to air and has an insoluble monolayer on the interface. Initially, everything is at rest, and the surfactant monolayer is uniformly distributed. At time $t = 0$, the bottom plate is set to oscillate with horizontal velocity $U \sin(2\pi\omega t)$. In this study, we consider the two-dimensional problem that is invariant in the transverse direction and neglect viscous coupling on the air side.

The governing equations are the two-dimensional Navier–Stokes equations, together with the continuity equation and appropriate boundary and initial conditions. It is convenient to use a streamfunction–vorticity formulation, where the nondimensional velocity vector and the corresponding (scalar) vorticity are

$$(u, v) = (\psi_y, -\psi_x), \quad \eta = -\psi_{xx} - \psi_{yy}.$$

We use H as the length scale and the viscous time H^2/ν as the time scale. The two-dimensional Navier–Stokes equations, with these scalings, reduce to the evolution equation for the vorticity:

$$\eta_t + \psi_y \eta_x - \psi_x \eta_y = \eta_{xx} + \eta_{yy}. \quad [1]$$

Initially, everything is at rest and the monolayer is uniformly spread; $\psi(x, y, 0) = \eta(x, y, 0) = 0$ and $c(x, 0) = c_0$. The boundary conditions on the solid boundaries are no-slip; for the two stationary vertical walls at $x = \pm L/H$, $\psi(\pm L/H, y, t) = \psi_x(\pm L/H, y, t) = 0$ and hence $\eta(\pm L/H, y, t) = -\psi_{xx}(\pm L/H, y, t)$. For the oscillating bottom, $\psi(x, 0, t) = 0$ and $\psi_y(x, 0, t) = \text{Re}_\alpha \sin(2\pi \text{Re}_\omega t)$; the two governing parameters are $\text{Re}_\alpha = UH/\nu$, the scaled velocity amplitude of the floor, and $\text{Re}_\omega = \omega H^2/\nu$, the scaled frequency of the floor oscillation. The vorticity is $\eta(x, 0, t) = -\psi_{yy}(x, 0, t)$. On

the air/water interface, being a material surface, $\psi(x, 1, t) = 0$ by continuity with its value on the sidewalls, which is set to zero without loss of generality. We assume that the interface is flat, and hence the contact angle at the air/water/solid contact line is 90° (in a physical laboratory experiment, the location of the contact line can be fixed by depositing a nonwetting paraffin film above the interface on the vertical walls (15); also, the Froude number, $\text{Fr} = v^2/gH^3$, for water at room temperature and a depth $H \sim 1$ cm, is only about 10^{-3}). This leaves the condition for the vorticity η on the interface to be specified.

We model the interface using the Boussinesq–Scriven constitutive relation (16). In planar two-dimensional systems with a flat interface, only the tangential stress balance plays a dynamic role (2). The tangential stress balance is, noting that at the interface $v = 0$:

$$\eta(x, 1, t) = -u_y(x, 1, t) = -C^{-1}\sigma_x - (\mathcal{B}u_x^s)_x, \quad [2]$$

where $C = \mu\nu/H\sigma_0$ is the capillary number, σ is the surface tension which varies with surfactant concentration c , $\sigma_0 = \sigma(c = 0)$, $\mathcal{B} = (\mu^s + \kappa^s)/\mu H$ is the Boussinesq number corresponding to the sum of the surface shear and dilatational viscosities (in general, also functions of c), scaled by μH , and $u^s(x, t) = u(x, 1, t)$. In (15), we determined that an insoluble monolayer comprised of vitamin K_1 , for concentrations up to 1 mg/m^2 , had negligible surface shear viscosity. In this study, we shall treat \mathcal{B} as constant since its functional dependence on c is not known a priori. This linearization is self-consistent as the computational results indicate that variations in c in both time and space are small for the parameter ranges considered. This reduces the surface viscosity term in Eq. [2] to $\mathcal{B}u_{xx}^s$. For $\sigma(c)$ we utilize the equation-of-state measured for water/vitamin K_1 in (15). This equation-of-state is plotted in Fig. 1, along with a

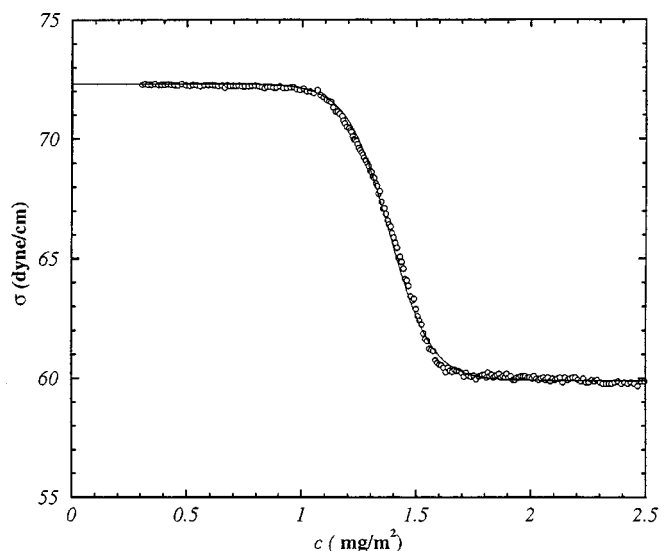


FIG. 1. Measured equation-of-state (open symbols) for a vitamin K_1 monolayer on air/water interface at 23°C (15), together with the curve fit given by Eq. [3].

fitted curve given by

$$\sigma = 66.1 + 6.2 \tanh(7.5(1 - c/1.38)). \quad [3]$$

Since the vorticity at the interface depends on surface tension gradients, which in turn depend on the surfactant concentration, we also need to solve an advection–diffusion equation for the surfactant concentration,

$$c_t + (c u^s)_x = \text{Pe}^{-1} c_{xx}, \quad [4]$$

where $\text{Pe} = \nu/D^s$ is the surface Peclet number and D^s is the diffusivity of the surfactant on the interface. Note that [4] is linear in c , so there is no need to nondimensionalize c . Conservation of insoluble surfactant on the interface is enforced with the zero-flux conditions $c_x(\pm L/H, t) = 0$. The zero-flux boundary condition assumed for insoluble monolayers is realizable in experiment for low Fr flow by pinning the contact line via the application of a nonwetting film on the sidewall above the waterline (15, 17).

The numerical solution of [1] and [4] together with the boundary and interface conditions follows that used in (15, 18). Specifically, a second-order centered finite-difference spatial discretization is used, with $n_x = 101$ and $n_y = 51$ grid points in the horizontal and vertical directions, respectively, together with a second-order predictor–corrector scheme for the time evolution. The time step, δt , is governed predominantly by the advection–diffusion Eq. [4] for the range of parameters chosen, and needs to be reduced when the surface velocity becomes small (which is the case when Marangoni stress is large and/or surface viscosities are large). The smallest value used was $\delta t = 10^{-7}$.

3. RESULTS

Equation [2] shows that the stress on the fluid at the interface is due to contributions from elasticity and surface viscosity. These contributions are qualitatively different in the way they relate to the thermodynamic state of the interface (via surfactant concentration) and its kinematics (fluid velocity at the interface), and their effects are complementary. To leading order, c is essentially constant (this is verified numerically for the Re_α and Re_ω ranges considered). The elastic term depends on the equation-of-state, as $\sigma_x = \sigma_c c_x$; for small c_x , its contribution is greatest for c values where the equation-of-state is steep, i.e., σ_c large, regardless of any velocity gradients. On the other hand, the surface viscosity term, $\mathcal{B}u_{xx}^s$, has \mathcal{B} essentially constant (for small c_x), but its contribution to the surface stress depends to leading order on surface velocity variations. These can be made large by appropriate oscillatory driving. Also, the elastic contribution dominates when there is large bulk inertia (flow) that drives a concentration gradient and results in a Marangoni stress that brings the surface velocity to zero. This occurs for adequately large Re_α and suitably small Re_ω . Whereas, the viscous contribution dominates when there are large surface velocity gradients, and is relatively insensitive to concentration gradients.

The objective of the computations presented here is to demonstrate that the flow under consideration is sensitive to surface viscosity effects in some range of parameter space. For this flow to provide a practical experimental technique to measure surface viscosities, \mathcal{B} , we need to show that it is sensitive to \mathcal{B} variations in a parameter regime accessible to laboratory measurements with a reasonable signal-to-noise ratio. We begin by noting that \mathcal{B} only appears in the tangential stress balance (2), and its effect on this balance may be completely masked by surface tension gradient effects. For a given surfactant system (and bulk liquid, e.g., water at room temperature), the only variable available to adjust the relative contributions of Marangoni stress and surface viscosities to the stress balance is the length scale H ; C^{-1} scales with H and \mathcal{B} scales with H^{-1} , so as H is reduced, the ratio of surface viscosity to elasticity is increased by H^{-2} . A practical lower limit is $H \sim 1$ cm, which would limit the Froude number to 10^{-3} and minimize surface deformations. For a vitamin K_1 monolayer on water of depth 1 cm at 23°C, this gives $C = 1.2 \times 10^{-6}$. In the present calculations, we have considered

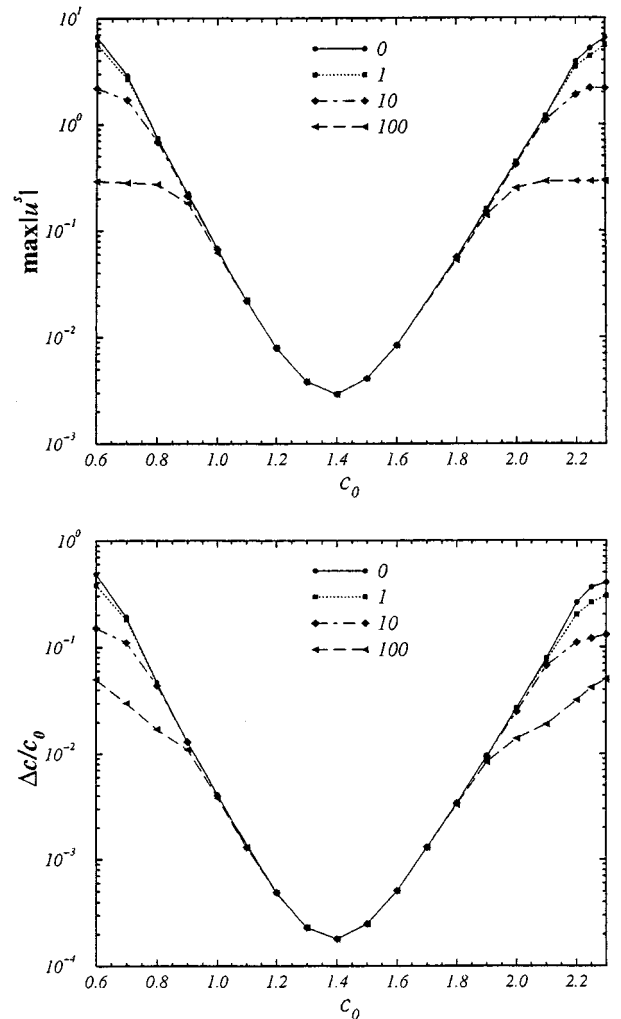


FIG. 2. Variation of $\max |u^s|$ and $\Delta c/c_0$ with c_0 (mg/m^2) for $\text{Re}_\alpha = 100$, $\text{Re}_\omega = 16$, $H/L = 1$, and \mathcal{B} as indicated.

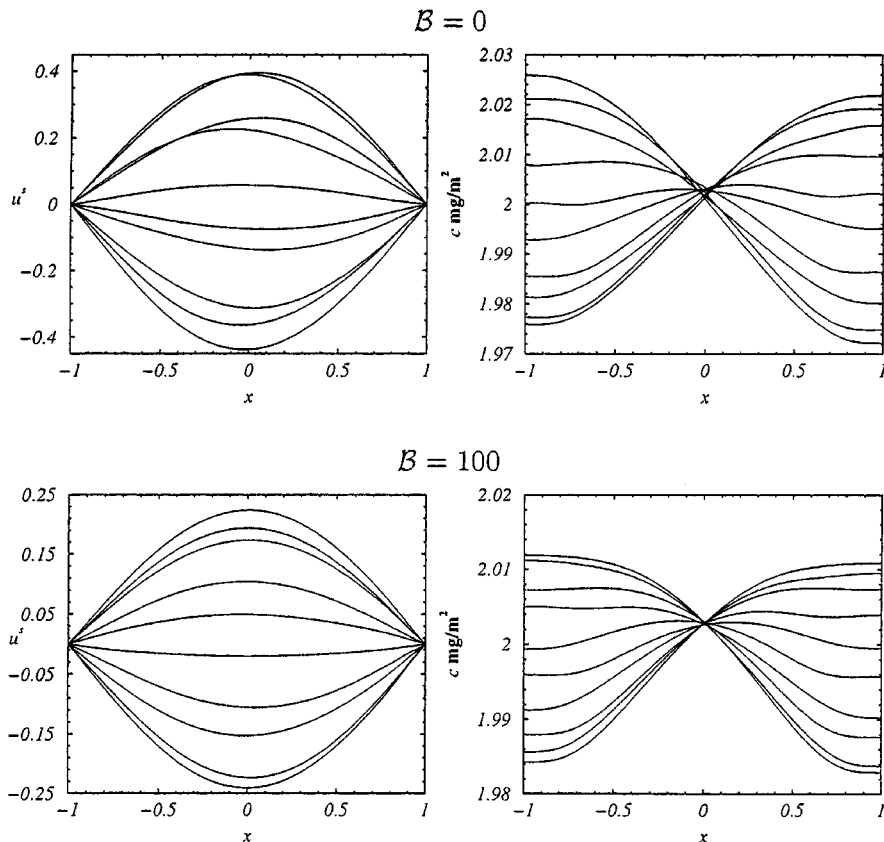


FIG. 3. Profiles of surface velocity, u^s , and concentration, c , at 10 phases over one oscillation period for $\text{Re}_\alpha = 100$, $\text{Re}_\omega = 16$, $H/L = 1$, $c_0 = 2.0 \text{ mg/m}^2$, and B as indicated.

various Re_α and Re_ω with c_0 up to 2.25 mg/m^2 , covering a large range of the equation-of-state. For each of these parameters, we have set $B = 0, 1, 10$, and 100 ; using our scalings, $B = 100$ corresponds to $(\mu^s + \kappa^s) = 0.9325 \text{ g/s}$ (surface Poise). In the calculations, we have set $\text{Pe} = 10$, which is probably about two orders of magnitude too small, but since the surfactant concentration gradients are everywhere small for the cases considered, we do not expect the results to be sensitive to Pe .

The flow geometry was selected to accentuate the contribution from surface viscosity. The parameters used to illustrate the results are selected with an eventual laboratory experiment in mind to verify the model and ultimately to measure the surface viscosities, B . The depth of the cavity, $H = 1 \text{ cm}$, was chosen to be as small as possible (in line with the above scaling argument), but not so small that Fr becomes large and surface flatness suffers, and surface velocity measurements are difficult. The frequency of oscillation, $\text{Re}_\omega = 16$, was selected to be large enough to avoid approaching a quasi-static monolayer ((18) showed that for steady flow, the effect of surface viscosities is very small at a steady monolayer front), yet small enough to give adequately large surface velocity and surface velocity gradients and avoid instabilities in the bulk flow. The amplitude of oscillation, $\text{Re}_\alpha = 100$, was selected to be large enough to ensure a strong surface flow (to keep viscosity in the bulk fluid from

diminishing the surface velocity) and small enough to avoid instabilities in the bulk flow (19). In Fig. 2, the maximum surface velocity over a complete period, $\max |u^s|$, and the relative change in concentration over a complete period, $\Delta c/c_0$, are plotted as functions of initial concentration, c_0 , for $B = 0, 1, 10$, and 100 in the driven cavity with $\text{Re}_\alpha = 100$, $\text{Re}_\omega = 16$, and $H/L = 1$, using a vitamin K_1 monolayer. The plot shows that over some ranges of c_0 , the effect of surface viscosity is to decrease the magnitude of the surface velocity, as expected. For $c_0 < 1$ or $c_0 > 1.8 \text{ mg/m}^2$, the change in surface velocity is well within the range that can be sensed in a laboratory measurement. The change in c is comparatively small, thus use of a constant surface viscosity in each calculation is justified.

Profiles of u^s and c over one period for a typical set of parameters ($\text{Re}_\alpha = 100$, $\text{Re}_\omega = 16$, $H/L = 1$, $c_0 = 2$) are presented in Fig. 3 for $B = 0$ and $B = 100$, illustrating the factor of two difference in u^s , which is detectable using now standard flow measuring techniques.

4. CONCLUSION

The theoretical foundations for a method for determining the surface dilatational viscosity of insoluble monolayers are presented (the planar geometry gives the sum of the surface shear

and dilatational viscosities and measurements of surface shear viscosity via independent established methods can be used to isolate the surface dilatational viscosity (20)). The time-periodic flow was chosen to minimize surface deformations and maximize gradients of surface velocity. By considering the nondimensionalized tangential stress balance, we show that the ratio of the surface viscosity term to the elastic term scales as H^{-2} , thus the cavity depth, H , needs to be minimized. Navier–Stokes computations are presented for a physical monolayer on the air/water interface; the equation-of-state for vitamin K_1 was used in the calculations since we have already demonstrated that it forms a well behaved monolayer and quantitative comparisons in a different flow between Navier–Stokes computations and measurements have already been made for this monolayer (15). For a range of surfactant concentration where surface elasticity is small, the method is sensitive down to order 10^{-2} surface Poise. With increasing surface viscosity, the range of concentration for which the viscosity can be determined increases. The flow geometry and operating conditions for the case presented correspond to conditions that are presently realizable in the laboratory, and produce a stable bulk flow. For these operating conditions, the computed amplitude of the maximum surface velocity is $40 \mu\text{m/s}$ in the absence of surface shear viscosity and $20 \mu\text{m/s}$ with surface viscosity of about 1 surface Poise (for a 1-cm-deep channel with water at room temperature). This difference is readily measurable by video microscopy of a tracer particle on the surface (5). Thus, this study suggests a practical method for determining surface viscosities, \mathcal{B} , consisting of the measurement of the motion of a tracer particle on the interface and comparisons with Navier–Stokes predictions at various values of \mathcal{B} .

ACKNOWLEDGMENT

This work was supported by NSF Grants CTS-9803478 and CTS-9896259.

REFERENCES

- Jiang, T.-S., Chen, J.-D., and Slattery, J. C., *J. Colloid Interface Sci.* **96**, 7 (1983).
- Edwards, D. A., Brenner, H., and Wasan, D. T., “Interfacial Transport Processes and Rheology.” Butterworth-Heinemann, London, 1991.
- Lopez, J. M., and Hirsra, A., *J. Colloid Interface Sci.* **206**, 231 (1998).
- Giermanska-Kahn, J., Monroy, F., and Langevin, D., *Phys. Rev. E* **60**, 7163 (1999).
- Maru, H. C., and Wasan, D. T., *Chem. Eng. Sci.* **34**, 1295 (1979).
- Li, D., and Slattery, J. C., *AICHE J.* **34**, 862 (1988).
- Avramidis, K. S., and Jiang, T. S., *J. Colloid Interface Sci.* **147**, 262 (1991).
- Hirsra, A., Korenowski, G. M., Logory, L. M., and Judd, C. D., *Langmuir* **13**, 3813 (1997).
- Kao, R. L., Edwards, D. A., Wasan, D. T., and Chen, E., *J. Colloid Interface Sci.* **148**, 247 (1992).
- Johnson, D. O., and Stebe, K. J., *J. Colloid Interface Sci.* **168**, 21 (1994).
- Tian, Y., Holt, R. G., and Apfel, R. E., *Phys. Fluids* **7**, 2938 (1995).
- Wantke, K.-D., and Fruhner, H., *J. Colloid Interface Sci.* **237**, 185 (2001).
- Holt, R. G., Tian, Y., Jankovsky, J., and Apfel, R. E., *J. Acoust. Soc. Am.* **102**, 3802 (1997).
- Maru, H. C., Mohan, V., and Wasan, D. T., *Chem. Eng. Sci.* **34**, 1283 (1979).
- Hirsra, A. H., Lopez, J. M., and Miraghaie, R., *J. Fluid Mech.* **443**, 271 (2001).
- Scriven, L. E., *Chem. Eng. Sci.* **12**, 98 (1960).
- Vogel, M. J., Hirsra, A. H., Kelley, J. S., and Korenowski, G. M., *Rev. Sci. Instr.* **72**, 1502 (2001).
- Lopez, J. M., and Hirsra, A., *J. Colloid Interface Sci.* **229**, 575 (2000).
- Shankar, P. N., and Deshpande, M. D., *Annu. Rev. Fluid Mech.* **32**, 93 (2000).
- Ting, L., Wasan, D. T., Miyano, K., and Xu, S.-Q., *J. Colloid Interface Sci.* **102**, 248 (1984).